

MICROSTRIP WIDEBAND BANDPASS FILTER WITH SIX TRANSMISSION ZEROS USING TRANSVERSAL SIGNAL-INTERACTION CONCEPTS

S. J. Xue^{1, 3}, W. J. Feng², H. T. Zhu³, and W. Q. Che^{2, 3 *}

¹University of Electronic Science and Technology of China, Chengdu 610054, China

²Department of Communication Engineering, Nanjing University of Science and Technology, Nanjing 210094, China

³State Key Laboratory of Millimeter Waves, City University of Hong Kong, Hong Kong, China

Abstract—A high-selectivity microstrip wideband bandpass filter with six transmission zeros using transversal signal-interaction concepts is proposed. A fifth-order wide passband with six transmission zeros ($0-2f_0$, f_0 is center frequency of the passband) can be realized two transmission paths. The bandwidth and locations of the transmission zeros can be adjusted conveniently by changing the characteristic impedances of open stub and coupling coefficients of the open/shorted coupled lines. A prototype of planar wideband bandpass filter with 3-dB fractional bandwidth 43.3% (2.33–3.63 GHz) is designed and fabricated. The measured and simulated results both indicate good performances of high selectivity and wideband harmonic suppression.

1. INTRODUCTION

Planar microstrip wideband bandpass filters with high selectivity and out-of-band rejection are extremely desirable in wide-band RF/microwave communication systems. In [1–8], multi-mode resonators, complementary split-ring resonator (CSRR), and multilayer aperture-coupled patches were used to design various microstrip wideband bandpass filters. In addition, electromagnetic (EM) loaded bandgap, the cascaded low-pass/high-pass filters, T-shaped resonators,

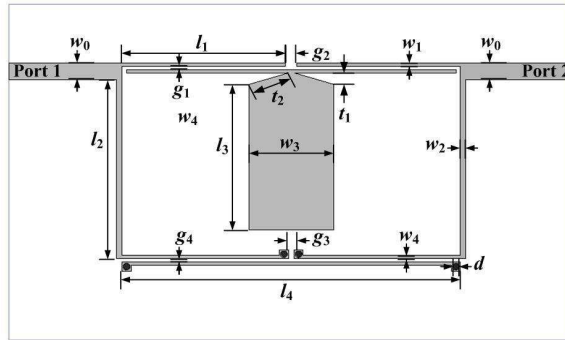
Received 28 September 2012, Accepted 16 October 2012, Scheduled 19 October 2012

* Corresponding author: Wen Quan Che (yeeren_che@163.com).

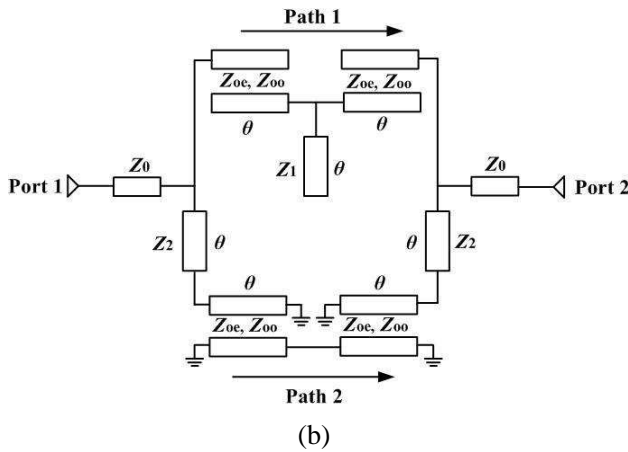
and stepped impedance resonators (SIR) were used to extend the upper stopband bandwidth and improve the selectivity of the passband [9–14].

Recently, microstrip wideband bandpass filters based on transversal signal-interaction concepts have drawn a lot of attention [15–21]. High-selectivity filtering characteristics with only a few resonators were realized in [15, 16], however, DC suppression was not solved and the circuit size should be further reduced. A wideband bandpass filter using transversal resonator and asymmetrical interdigital coupled lines with a good out-of-band response was realized in [17]. Another wideband bandpass filters with an ideal DSPSL (double-sided parallel-strip line) 180 phase inversion was introduced in [18]. The filter has high selectivity and good harmonic suppression; however, two via holes were used to realize the ideal 180 swap, causing fabrication difficulty. Moreover, two wideband bandpass filters based on the ideal 180° phase inversion of the two shorted coupled lines were proposed in [19, 20]. However, there is only one transmission zero (in the upper stopband) closed to the passband, and the 3-dB bandwidth of the filters is not easy to adjust. In [21], another new wideband bandpass filter using Marchand balun based on transversal signal-interaction concepts was introduced, indicating some advantages of compact circuit size, adjustable bandwidth and high selectivity. Moreover, we also proposed several wideband balanced circuits using transversal signal-interaction concepts in [22, 23], wide passband for the differential mode and wideband common mode suppressed can be easily achieved due to signals superposition of different transmission paths.

In this paper, a new microstrip high-selectivity wideband bandpass filter using transversal signal-interaction concepts based on T-shaped structure [13] and open/shorted coupled lines is proposed. Six transmission zeros ($0-2f_0$, f_0 is the centre frequency of the passband) can be realized due to the superposition of signals of the two transmission paths with a T-shaped structure and open/shorted coupled lines. A prototype of wideband bandpass filter operating at 3.0 GHz with fifth-order passband is designed. All the structures are simulated with Ansoft HFSS v.11.0 and constructed on Rogers 5880 with dielectric constant 2.2 and thickness 0.508 mm, and $\tan \delta = 0.0009$. Detailed theoretical design, simulation and experimental results are demonstrated and discussed.



(a)



(b)

Figure 1. (a) Top view of the microstrip wideband bandpass filter. (b) Equivalent circuit of the microstrip wideband bandpass filter.

2. DESIGN OF THE PROPOSED MICROSTRIP BANDPASS FILTER

2.1. Basic Theoretical Analysis

Figures 1(a) and (b) show the top view and the equivalent circuit of the microstrip wideband bandpass filter. Two different transmission paths are introduced to realize the signal transmission from Port 1 to Port 2. For Path 1, a T-shaped structure (characteristic impedance Z_1 , electrical length θ , $\theta = 90^\circ$ at the center frequency f_0) is located in the center of the two open coupled lines (even/odd-mode characteristic impedance Z_{oe} and Z_{oo} , electrical length θ). For Path 2, two shorted

coupled lines (even/odd-mode characteristic impedance Z_{oe} and Z_{oo} , electrical length θ) are connected in the center of the two transmission lines with characteristic impedance Z_2 and electrical length θ . In addition, the characteristic impedances of the two microstrip lines at the input/output ports are all $Z_0 = 50 \Omega$.

The $ABCD$ matrices of the open stub, transmission lines and open/shorted coupled lines are [24]:

$$\begin{aligned}
 M_{stub} &= \begin{bmatrix} 1 & 0 \\ j \tan \theta / Z_1 & 1 \end{bmatrix}, & M_{line} &= \begin{bmatrix} \cos \theta & j Z_2 \sin \theta \\ j Y_2 \sin \theta & \cos \theta \end{bmatrix} \\
 M_o &= \begin{bmatrix} \frac{Z_{oe} + Z_{oo}}{Z_{oe} - Z_{oo}} \cos \theta & j \frac{(Z_{oe} - Z_{oo})^2 - (Z_{oe} + Z_{oo})^2 \cos^2 \theta}{2(Z_{oe} - Z_{oo}) \sin \theta} \\ j \frac{2 \sin \theta}{Z_{oe} - Z_{oo}} & \frac{Z_{oe} + Z_{oo}}{Z_{oe} - Z_{oo}} \cos \theta \end{bmatrix} \\
 M_s &= \begin{bmatrix} \frac{Y_{oe} + Y_{oo}}{Y_{oe} - Y_{oo}} \cos \theta & j \frac{2 \sin \theta}{Y_{oe} - Y_{oo}} \\ j \frac{2 Y_{oe} Y_{oo} \cos \theta \cot \theta}{Y_{oo} - Y_{oe}} - j \frac{(Y_{oo} - Y_{oe}) \sin \theta}{2} & \frac{Y_{oe} + Y_{oo}}{Y_{oe} - Y_{oo}} \cos \theta \end{bmatrix}
 \end{aligned} \tag{1}$$

For Path 1, the $ABCD$ matrix is $M_o \times M_{stub} \times M_o$ (M_o — open coupled line, M_{stub} — open stub Z_1); for Path 2, the $ABCD$ matrix is $M_{line} \times M_s \times M_s \times M_{line}$ (M_{line} — transmission line Z_2 , M_s — shorted coupled line). After the $ABCD$ - and Y -parameter conversions, the S -parameters of the wideband bandpass filter can be illustrated as [24]:

$$S_{11} = \frac{Y_o^2 - Y_{11}^2 + Y_{21}^2}{(Y_o + Y_{11})(Y_o + Y_{22}) - Y_{12} Y_{21}}, \quad S_{21} = \frac{-2 Y_{21} Y_o}{(Y_o + Y_{11})(Y_o + Y_{22}) - Y_{12} Y_{21}} \tag{2}$$

And $Y = 1/Z$ ($Z_0 = 50 \Omega$), when $S_{21} = 0$ ($Y_{21} = 0$), the transmission zeros of the circuit of Figure 1(b) can be obtained:

$$\begin{aligned}
 \theta_{tz1} &= 0, & \theta_{tz6} &= \pi \\
 \theta_{tz2} &= \arccos \sqrt{\frac{1 + \sqrt{1 - (1 - \sqrt{\frac{cd}{ab}})}}{2}}, & \theta_{tz5} &= \pi - \theta_{tz2} \\
 \theta_{tz3} &= \arccos \sqrt{\frac{1 - \sqrt{1 - (1 - \sqrt{\frac{cd}{ab}})}}{2}}, & \theta_{tz4} &= \pi - \theta_{tz3} \\
 a &= \frac{Z_2^2 (Z_{oe} + Z_{oo})}{Z_{oe} Z_{oo}} - \frac{4 (Z_{oe} + Z_{oo}) (Z_{oe} Z_{oo} + Z_{oe} Z_2 + Z_{oo} Z_2 - Z_1^2)}{(Z_{oe} - Z_{oo})^2} \\
 b &= -2 (Z_{oe} + Z_{oo}) - \frac{4 Z_{oe} Z_{oo}}{Z_1} - \frac{(Z_{oe} - Z_{oo})^2}{2 Z_1} \\
 &\quad - \frac{8 Z_{oe} Z_{oo} (Z_{oe} Z_{oo} + Z_{oe} Z_1 + Z_{oo} Z_1)}{Z_1 (Z_{oe} - Z_{oo})^2}
 \end{aligned} \tag{3}$$

$$\begin{aligned}
 c &= \frac{4(Z_{oe}+Z_{oo})(Z_{oe}Z_{oo}+Z_{oe}Z_2+Z_{oo}Z_2)}{Z_1(Z_{oe}-Z_{oo})^2} - \frac{Z_2^2(Z_{oe}+Z_{oo})}{Z_{oe}Z_{oo}} + 4Z_2 \\
 &+ \frac{(Z_{oe}-Z_{oo})^2}{Z_1} - \frac{16Z_{oe}Z_{oo}(Z_{oe}Z_{oo}+Z_{oe}Z_1+Z_{oo}Z_1)}{Z_1(Z_{oe}-Z_{oo})^2} \\
 &+ \frac{4(Z_{oe}+Z_{oo})(Z_{oe}Z_{oo}+Z_{oe}Z_2+Z_{oo}Z_2)}{Z_1(Z_{oe}-Z_{oo})^2} - \frac{Z_2^2(Z_{oe}+Z_{oo})}{Z_{oe}Z_{oo}} \\
 d &= 2(Z_{oe}+Z_{oo}) + \frac{4Z_{oe}Z_{oo}}{Z_1} - \frac{(Z_{oe}-Z_{oo})^2}{2Z_1} \\
 &- \frac{8Z_{oe}Z_{oo}(Z_{oe}Z_{oo}+Z_{oe}Z_1+Z_{oo}Z_1)}{Z_1(Z_{oe}-Z_{oo})^2} \\
 &+ \frac{4(Z_{oe}+Z_{oo})(Z_{oe}Z_{oo}+Z_{oe}Z_2+Z_{oo}Z_2)}{Z_1(Z_{oe}-Z_{oo})^2} + \frac{Z_2^2(Z_{oe}+Z_{oo})}{Z_{oe}Z_{oo}} - 4Z_2
 \end{aligned} \tag{4}$$

The solutions $\theta_{tz} = 0, \pi$ correspond to 0 and $2f_0$, respectively, which are the inherent transmission zeros of the open/shorted coupled lines [24]. In addition, the transmission poles in the passband can be calculated when $S_{11} = 0$, saying, a fifth-order equation for θ versus Z_1, Z_2, Z_{oe} and Z_{oo} can be obtained for this case. When Z is fixed, five roots for $S_{11} = 0$ can be acquired by proper choosing the relationships of Z_1, Z_2, Z_{oe} and Z_{oo} , and then five transmission poles in the passband can be achieved.

Figures 2(a)–(b) show the simulated results of the circuit in Figure 1(b). Due to the superposition of signals for Paths 1 and 2, four transmission zeros ($f_{tz2}, f_{tz3}, f_{tz4}, f_{tz5}$) can be easily achieved,

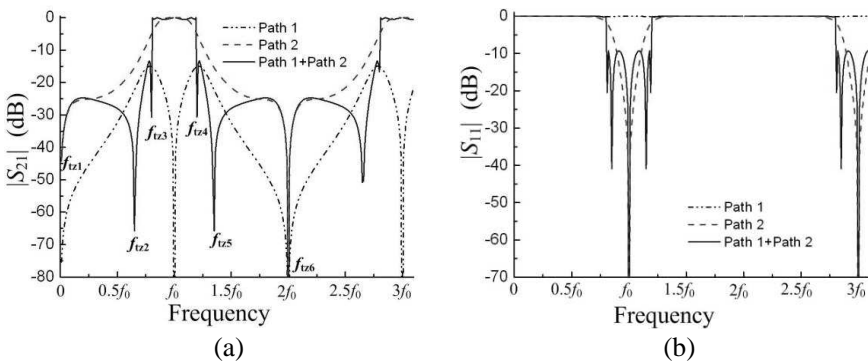


Figure 2. (a) $|S_{21}|$ of Figure 1(b), $Z_1 = 12 \Omega, Z_2 = 100 \Omega, Z_{oe} = 185 \Omega, Z_{oo} = 85 \Omega$. (b) $|S_{11}|$ of Figure 1(b), $Z_1 = 12 \Omega, Z_2 = 100 \Omega, Z_{oe} = 185 \Omega, Z_{oo} = 85 \Omega$.

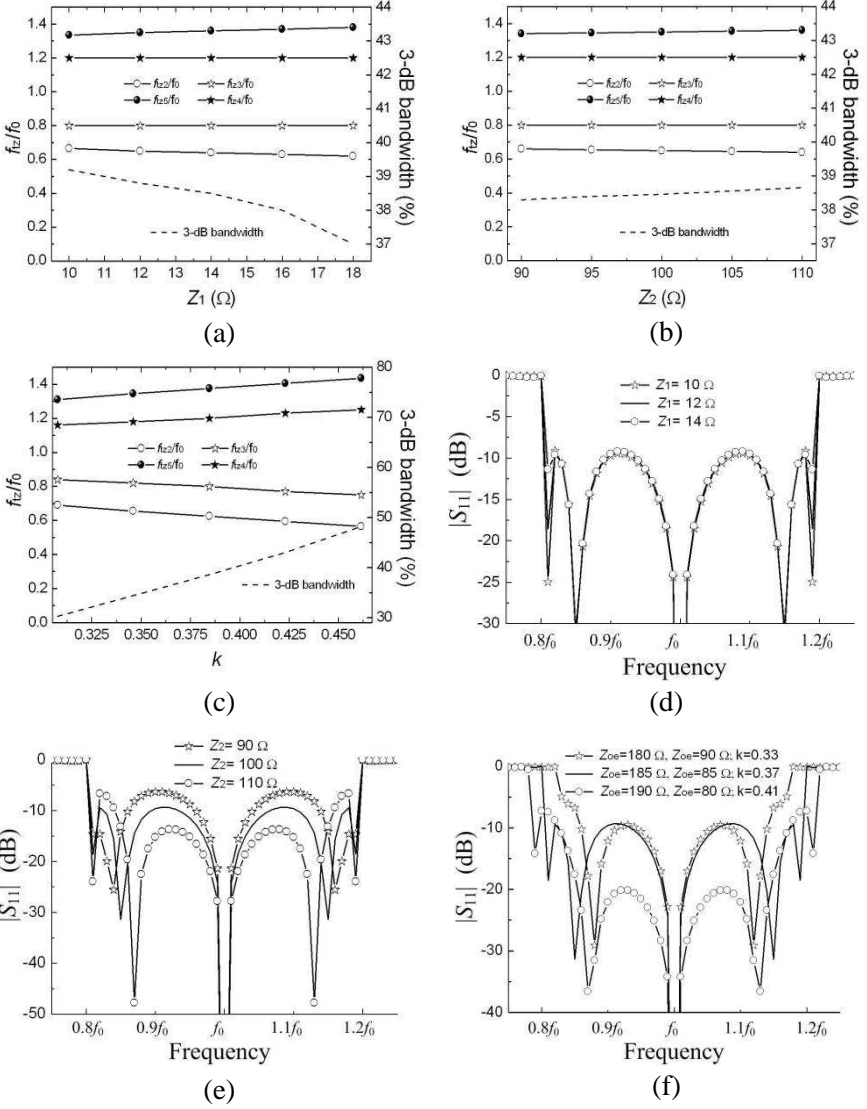


Figure 3. (a) f_{tz2} , f_{tz3} , f_{tz4} , f_{tz5} and 3-dB bandwidth versus Z_1 , $Z_2 = 110 \Omega$, $Z_{oe} = 185 \Omega$, $Z_{oo} = 85 \Omega$. (b) f_{tz2} , f_{tz3} , f_{tz4} , f_{tz5} and 3-dB bandwidth versus Z_2 , $Z_1 = 14 \Omega$, $Z_{oe} = 185 \Omega$, $Z_{oo} = 85 \Omega$. (c) f_{tz2} , f_{tz3} , f_{tz4} , f_{tz5} and 3-dB bandwidth versus k , $Z_1 = 14 \Omega$, $Z_2 = 110 \Omega$. (d) $|S_{11}|$ versus Z_1 , $Z_2 = 100 \Omega$, $Z_{oe} = 185 \Omega$, $Z_{oo} = 85 \Omega$. (e) $|S_{11}|$ versus Z_2 , $Z_1 = 12 \Omega$, $Z_{oe} = 185 \Omega$, $Z_{oo} = 85 \Omega$. (f) $|S_{11}|$ versus k , $Z_1 = 14 \Omega$, $Z_2 = 100 \Omega$.

leading to a quasi-elliptic function that improves the passband and out-of-band performances for the wideband bandpass filter. The five in-band transmission poles reflect the fact that $S_{11} = 0$ has five real solutions when Z_1 , Z_2 , Z_{oe} and Z_{oo} are properly selected.

In addition, when Z_0 and θ are fixed, three variables Z_1 , Z_2 , and k ($k = (Z_{oe} - Z_{oo}) / (Z_{oe} + Z_{oo})$) need to be determined by taking into account not only the characteristics of the filter but also the tunability of the passband. Figures 3(a), (b), (c), (d), (e), and (f) show the transmission zeros (f_{tz2} , f_{tz3} , f_{tz4} , f_{tz5}), 3-dB bandwidth and $|S_{11}|$ versus different characteristic impedance Z_1 , Z_2 and k ($k = (Z_{oe} - Z_{oo}) / (Z_{oe} + Z_{oo})$). We may see that, the transmission zeros f_{tz2} and f_{tz5} move away from f_0 as Z_1 , Z_2 and k increase; the transmission zeros f_{tz3} and f_{tz4} move away from f_0 as k increases, and the 3-dB bandwidth of the passband decreases as Z_1 , increases as Z_2 and k increase, in addition, the in-band balance can be also adjusted by Z_1 , Z_2 and k . In this way, the performances of the wideband bandpass filter can be controlled conveniently by changing the characteristic impedances Z_1 , Z_2 , Z_{oe} and Z_{oo} when Z_0 and θ are fixed. Actually, the 3-dB bandwidth of the passband can be illustrated as $f_{3dB} = f(Z_{oe}, Z_{oo}, Z_1, Z_2)$. Once Z_0 and θ are determined, we can adjust Z_{oe} , Z_{oo} , Z_1 and Z_2 to satisfy the demand of 3-dB bandwidth f_{3dB} , and the transmission characteristic for the passband can be simultaneously obtained and further optimized based on the above discussion.

2.2. Proposed Microstrip Wideband Bandpass Filter

To clarify the proposed filter design, the design procedures of wideband bandpass filter are summarized as follows:

(1) Based on the Equations (1)–(4), choose the desired 3-dB bandwidth f_{3dB} of the bandpass filter, determine the values Z_1 , Z_2 , Z_{oe} and Z_{oo} to meet fifth-order passband with six transmission zeros from the response up to $2f_0$;

(2) Adjust the values of Z_1 , Z_2 , Z_{oe} and Z_{oo} to determine the locations of the four transmission zeros (f_{tz2} , f_{tz3} , f_{tz4} , f_{tz5}) from 0 to $2f_0$; when Z_0 and θ are determined, further optimize the values of Z_1 , Z_2 , Z_{oe} and Z_{oo} to realize better in-band and out-of-band transmission characteristics of the wideband filter.

Based on the above theoretical analysis, the final parameters for the filter circuit of Figure 1(b) are given as follows: $Z_0 = 50 \Omega$, $Z_1 = 12 \Omega$, $Z_2 = 100 \Omega$, $Z_{oe} = 185.6 \Omega$, $Z_{oo} = 84.6 \Omega$, $f_0 = 3.0 \text{ GHz}$. The simulated results of the microstrip wideband bandpass filter in Figure 1(a) ($0.70\lambda_g \times 0.40\lambda_g$, $l_1 = 18.7 \text{ mm}$, $l_2 = 18.7 \text{ mm}$, $l_3 = 16.6 \text{ mm}$, $l_4 = 38.4 \text{ mm}$, $w_0 = 1.5 \text{ mm}$, $w_1 = 0.2 \text{ mm}$, $w_2 = 0.47 \text{ mm}$, $w_3 = 9.2 \text{ mm}$, $w_4 = 0.2 \text{ mm}$, $t_1 = 1.0 \text{ mm}$, $t_2 = 4.4 \text{ mm}$, $g_1 = 0.2 \text{ mm}$,

$g_2 = 0.15$ mm, $g_3 = 0.5$ mm, $g_4 = 0.15$ mm, $d = 0.5$ mm) are shown in Figure 4. Obviously, the simulated insertion loss is less than 0.5 dB while the return loss is over 10 dB from 2.35 GHz to 3.63 GHz (3-dB bandwidth is approximately 44.1%, 2.33–3.65 GHz). Six transmission zeros are located at 0, 1.68, 2.3, 3.66, 4.34 and 5.85 GHz with a fifth-order passband are realized to improve the selectivity and harmonic suppression. Furthermore, over 20-dB upper stopband is achieved from 3.95 GHz to 7.95 GHz ($2.65f_0$). The group delay is less than 1.0 ns in the whole passband.

3. MEASURED RESULTS AND DISCUSSIONS

Figure 4(a) illustrates the photograph of the microstrip wideband bandpass filter with six transmission zeros from 0 to $2f_0$, which is designed on Rogers 5880 with dielectric constant 2.2 and thickness 0.508 mm. The efficient electric size of the proposed filter is $0.70\lambda_g \times 0.40\lambda_g$. The measured S -parameters and the group delay are illustrated in Figures 4(b). Good agreement can be found between the measured and simulated results. Six transmission zeros are found to locate at 0, 1.66, 2.3, 3.64, 4.22 and 5.96 GHz, respectively; a sixth-order passband with insertion loss less than 1.1 dB while return loss over 11 dB from 2.36 GHz to 3.62 GHz is realized. Furthermore, over 20-dB upper stopband is achieved from 3.92 GHz to 8.02 GHz ($2.67f_0$). The measured group delay is less than 1.0 ns from 2.6 GHz to 3.36 GHz. The slight frequency discrepancies between the measured and simulated results are mainly caused by the limited fabrication precision and measurement errors.

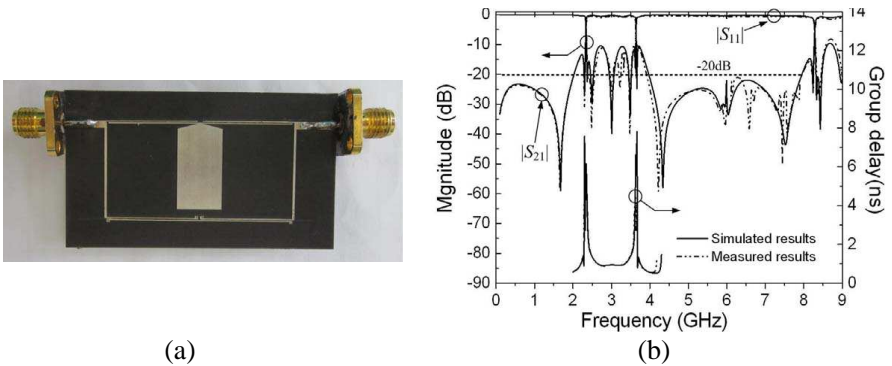


Figure 4. (a) Photograph of the microstrip wideband bandpass filter. (b) Measured and simulated results of the wideband bandpass filter.

Table 1. Comparisons of measured results for several wideband filters.

Filter Structures	Transmission zeros ($ S_{21} $, $0-2f_0$)	Transmission poles ($ S_{11} $, in-band)	$\Delta f_{3\text{dB}}(\%)$	Upper stopband (dB)	Group delay (ns)
Ref. [15]	6	1	10.7%	> 15 ($1.4f_0$)	-
Ref. [16]	6	3	27.6%	> 15 ($1.5f_0$)	< 0.70
Ref. [17]	4	5	75%	> 20 ($2.5f_0$)	< 0.70
Ref. [18]	4	4	123%	> 20 ($2.3f_0$)	< 1.50
Ref. [19]	3	3	117.6%	> 15 ($2.4f_0$)	< 0.50
Ref. [20]	4	3	124.6%	> 15 ($2.5f_0$)	< 0.30
Ref. [21]	4	3	110%	> 13 ($2.4f_0$)	< 0.60
This work	6	6	43.3%	> 20 ($2.67f_0$)	< 1.0

To further demonstrate the performances of the filters, the comparisons of measured results for several wideband filter structures [15–21] are shown in Table 1. The proposed wideband bandpass filter has more transmission zeros to further improve the passband selectivity and harmonic suppression compared with the other wideband filter structures in [15–21], and the upper stopband of the proposed wideband bandpass filter stretches up to $2.67f$ due to the multiple transmission zeros in out-of-band. Moreover, to extend the upper stopband, some lowpass/bandstop networks can be cascaded to further improve the upper stopband performance of the two wideband bandpass filters [9–14], and to achieve tighter coupling and wider passband for the filter, patterned ground-plane technology [21, 22] can be used in the proposed wideband bandpass filter.

4. CONCLUSION

A microstrip high-selectivity wideband bandpass filter using transversal signal-interaction concepts is designed and fabricated. Six transmission zeros with a fifth-order passband are achieved to improve the selectivity and harmonic suppression of the filter. Compared with former wideband differential structures [15–21], the proposed wideband filter has higher selectivity and wider-band harmonic suppression. Good agreements between simulated and measured responses of the filter are demonstrated, indicating the validity of the design strategies.

ACKNOWLEDGMENT

This work is supported by the National Natural Science Foundation of China (60971013), 2010 Graduate Innovative Project of Jiangsu Province (CX10B.125Z), China, and in part by the Major State Basic Research Development Program of China (973 Program: 2009CB320201).

REFERENCES

1. Zhu, L., S. Sun, and W. Menzel, "Ultra-wideband (UWB) bandpass filter using multiple-mode resonator," *IEEE Microw. Wireless Compon. Lett.*, Vol. 15, No. 11, 796–798, Nov. 2005.
2. Xiao, J.-K. and Y. Li, "Novel compact microstrip square ring bandpass filter," *Journal of Electromagnetic Waves and Applications*, Vol. 20, No. 13, 1817–1826, 2006.
3. Kharakhili, F. G., M. Fardis, G. Dadashzadeh, and A. Ahmadi, "Circular slot with a novel circular microstrip open ended microstrip feed for UWB applications," *Progress In Electromagnetics Research*, Vol. 68, 161–167, 2007.
4. Chu, H. and X. Q. Shi, "Compact ultra-wideband bandpass filter based on SIW and DGS technology with a notch band," *Journal of Electromagnetic Waves and Applications*, Vol. 25, No. 4, 589–596, 2011.
5. Lai, X., Q. Li, P. Y. Qin, B. Wu, and C. H. Liang, "A novel wideband bandpass filter based on complementary split-ring resonator," *Progress In Electromagnetics Research C*, Vol. 1, 177–184, 2008.
6. Razalli, M. S., A. Ismail, M. A. Mahdi, and M. N. Hamidon, "Novel compact microstrip ultra-wideband filter utilizing short-circuited stubs with less vias," *Progress In Electromagnetics Research*, Vol. 88, 91–104, 2008.
7. Wei, F., L. Chen, X.-W. Shi, X. H. Wang, and Q. Huang, "Compact UWB bandpass filter with notched band," *Progress In Electromagnetics Research C*, Vol. 4, 121–128, 2008.
8. Wu, Y., Y. Liu, S. Li, and C. Yu, "A simple microstrip bandpass filter with analytical design theory and sharp shirt selectivity," *Journal of Electromagnetic Waves and Applications*, Vol. 25, Nos. 8–9, 1253–1263, 2011.
9. Gao, S. S., S. Q. Xiao, J. P. Wang, X.-S. Yang, Y. X. Wang, and B. Z. Wang, "A compact UWB bandpass filter with wide

- stopband,” *Journal of Electromagnetic Waves and Applications*, Vol. 22, Nos. 8–9, 1043–1049, 2008.
10. Lin, W. J., C. S. Chang, J. Y. Li, D. B. Lin, L. S. Chen, and M. P. Houg, “Improved compact broadband bandpass filter using branch stubs co-via structure with wide stopband characteristic,” *Progress In Electromagnetics Research C*, Vol. 5, 45–55, 2008.
 11. Shobeyri, M. and M. H. Vadjed-Samiei, “Compact ultra-wideband bandpass filter with defected ground structure,” *Progress In Electromagnetics Research Letters*, Vol. 4, 25–31, 2008.
 12. Feng, W. J. and W. Q. Che, “Novel wideband differential bandpass filter based on T-shaped structure,” *IEEE Trans. Microw. Theory Tech.*, Vol. 6, No. 60, 1560–1568, 2012.
 13. Lin, W. J., J. Y. Li, D. B. Lin, L. S. Chen, and M. P. Houg, “Miniaturized wideband ring-type bandpass filters with upper stopband characteristic,” *Journal of Electromagnetic Waves and Applications*, Vol. 24, No. 7, 931–939, 2010.
 14. Gao, M. J., L. S. Wu, and J. F. Mao, “Compact notched ultra-wideband bandpass filter with improved out-of-band performance using quasioelectromagnetic bandstop structure,” *Progress In Electromagnetics Research Letters*, Vol. 125, 137–150, 2012.
 15. Gómez-García, R., J. I. Alonso, and D. Amor-Martn, “Using the branchline directional coupler in the design of microwave bandpass filters,” *IEEE Trans. Microw. Theory Tech.*, Vol. 10, No. 53, 3221–3229, 2005.
 16. Gómez-García, R. and J. I. Alonso, “Design of sharp-rejection and low-loss wide-band planar filters using signal-interference techniques,” *IEEE Microw. Wireless Compon. Lett.*, Vol. 8, No. 15, 530–5327, 2005.
 17. Sun, S., L. Zhu, and H. H. Tian, “A compact wideband bandpass filter using transversal resonator and asymmetrical interdigital coupled lines,” *IEEE Microw. Wireless Compon. Lett.*, Vol. 3, No. 18, 173–1755, 2008.
 18. Wong, K. W., L. Chiu, and Q. Xue, “Wideband parallel-strip bandpass filter using phase inverter,” *IEEE Microw. Wireless Compon. Lett.*, Vol. 8, No. 18, 503–505, 2008.
 19. Feng, W. J. and W. Q. Che, “Novel ultra-wideband bandpass filter using shorted coupled lines and transversal transmission line,” *IEEE Microw. Wireless Compon. Lett.*, Vol. 10, No. 20, 548–551, 2010.
 20. Sánchez-Soriano, M. A., E. Bronchalo, and G. Torregrosa-Penalva, “Compact UWB bandpass filter based on signal interference

- techniques,” *IEEE Microw. Wireless Compon. Lett.*, Vol. 11, No. 19, 692–694, 2009.
21. Feng, W. J., W. Q. Che, and T. F. Eibert, “Ultra-wideband bandpass filter based on transversal signal-interaction concepts,” *Electron. Lett.*, Vol. 24, No. 47, 1330–1331, 2011.
 22. Zhu, H. T., W. J. Feng, W. Q. Che, and Q. Xue, “Ultra-wideband differential bandpass filter based on transversal signal-interference concept,” *Electron. Lett.*, Vol. 18, No. 47, 1033–1034, 2011.
 23. Feng, W. J., W. Q. Che, T. F. Eibert, and Q. Xue, “Compact differential ultra-wideband bandpass filter based on the double-sided parallel-strip line and transversal signal-interaction concepts,” *IET Microwaves, Antennas and Propagation*, Vol. 2, No. 6, 186–195, 2012.
 24. Matheai, G. L., L. Young, and E. M. T. Jones, *Microwave Filters, Impedance-matching Networks, and Coupling Structures*, Artech House, Dedham, 1980.